Long non-coding RNA transcribed from pseudogene PPIAP43 is associated with radiation sensitivity of small cell lung cancer cells

SHILONG WANG[1,2] and JINMING YU[2,3]

[1]Cheeloo College of Medicine, Shandong University, Jinan, Shandong 250012;
[2]Department of Radiation Oncology, Shandong Cancer Hospital Affiliated to Shandong University;
[3]Department of Radiation Oncology, Shandong Cancer Hospital and Institute, Shandong Academy of Medical Sciences, Jinan, Shandong 250117, P.R. China

Received February 20, 2019; Accepted July 26, 2019

DOI: 10.3892/ol.2019.10806

Abstract. Small cell lung cancer (SCLC) is a highly lethal disease. Although radiation therapy is effective for the majority of patients with SCLC, patient sensitivity to radiation varies. The lack of biomarkers impedes advances in targeting radiation-sensitive patients. In this study, the changes in transcription patterns of SCLC cell lines were evaluated with or without 2 Gy gamma radiation. The results demonstrated that peptidyl-prolyl cis-trans isomerase A pseudogene 43 (PPIAP43) transcription was increased 2-fold in cells irradiated with 2 Gy gamma radiation compared with unirradiated cells in pre-reported radio-sensitive sensitive cell lines H69, H128, H146, H209 and H187. These cells shared 259 upregulated and 96 downregulated RNA transcripts following radiation. Pre-reported less sensitive cell lines H526, D53, D114 and D153 in which PPIAP43 was not upregulated 2-fold following irradiation with 2 Gy gamma radiation compared with unirradiated cells, shared 3 upregulated and 9 downregulated RNA transcripts. The RNA transcript of PPIAP43 was aligned with the mRNA of peptidyl-prolyl cis-trans isomerase A (PPIA) at 2 sections (3,732 to 3,917 and 5,327 to 5,657 of the PPIA gene) and the sequences were shown to be 96 and 94% similar, respectively. Therefore, PPIAP43 may act as a sponge for microRNAs which bind with the RNA of PPIA. Therefore, PPIAP43 RNA transcription may serve as a potential biomarker of radio-sensitivity of SCLC.

Correspondence to: Dr Jinming Yu, Department of Radiation Oncology, Shandong Cancer Hospital Affiliated to Shandong University, 440 Jiyan Road, Jinan, Shandong 250117, P.R. China
E-mail: sdyujinming@163.com

Abbreviations: SCLC, small cell lung cancer; RT, radiation therapy; PPIA, peptidyl-prolyl cis-trans isomerase A; PPIAP43, peptidyl-prolyl cis-trans isomerase A pseudogene 43; miRNA, micro RNA; lncRNA, long non-coding RNA; GO, Gene Ontology; DEG, differentially expressed gene; BLAST, Basic Local Alignment Searching Tool; DAVID, the Database for Annotation, Visualization and Integrated Discovery; KEGG, Kyoto Encyclopedia of Genes and Genomes; ARHGAP42, Rho GTPase activating protein 42; PPIAL4A, peptidyl-prolyl cis-trans isomerase A like 4A.

Key words: small cell lung cancer cell lines, radiation sensitivity, potential biomarker, PPAP43, Cyclophilin A

Introduction

Small cell lung cancer (SCLC) is a highly malignant cancer. According to a recent review, SCLC accounts for approximately 15% of cases of lung cancers in the USA (2014), UK (2014), China (2014) and Korea (2016) (1). Regardless of the progression of the treatment for the other types of lung cancer, such as targeted therapy and immunotherapy, the most common therapeutic options for SCLC are traditional chemotherapy, radiation therapy (RT) and surgical therapy (2). The outcome of SCLC has not improved considerably, and the five-year survival of SCLC is only 7% (1). Thus, besides pioneering new therapies, modification of traditional ones is needed, and radiation therapy as a major treatment option for SCLC needs to be refined.

The effects of RT include undesirable side effects on normal tissues (3). Normally, a higher curative effect and a lower side effect are desirable. Advanced technologies such as intensity-modulated and stereotactic body RT can limit the irradiation area (4,5); however, to further avoid damage to normal tissue, it is important to determine whether the cancer cells are sensitive to radiation as early as possible. At present, there are no biomarkers in clinical use for predicting the effectiveness of RT on certain types of the disease.

Next generation sequencing (NGS) technology provides high throughput data of gene-transcribed mRNAs and RNAs transcribed from the non-coding regions. The National Center for Biotechnology Information (NCBI) Gene Expression Omnibus (GEO) database enables mass exploration of data to obtain precise and comprehensive information on diseases. With these tools, the present study aimed to find a potential biomarker for prediction the effectiveness of radiation therapy on SCLC by mining in the databases.

Materials and methods

Datasets. The gene expression data GSE55830 was collected from NCBI GEO datasets (6). This dataset comprises data of different SCLC cell lines (H69, H128, H146, H209, H187, H526,

D53, D114 and D153) treated with various therapeutic methods including radiation therapy and chemotherapy, as well as controls. The experiment was based on Illumina HumanHT-12 V4.0 expression beadchip (GPL10558). BRB-ArrayTools integrated in Excel 2016 (Microsoft Corporation) was used to display the data with default parameters (7).

Identification of the underlying targets. The 'Array vs. Array' module in BRB-ArrayTools was used to display the differentially expressed sequences between radiation-treated and the control arrays of each cell line on a log2 scale.

Classification of differentially expressed genes (DEGs). Cell lines were divided into two groups with a cut-off of 2-fold transcription change of the chosen sequence in the former step. Each cell line was respectively categorized as group A when the transcription levels of PPIAP43 were increased ≥2 fold following 2 Gy gamma radiation compared with the unirradiated control cells, or group B when the transcription levels of PPIAP43 were decreased or increased <2 fold following 2 Gy gamma radiation compared with the unirradiated control cells. The two groups were processed by the class comparison module between controls and radiation groups paired by cell line names.

Functional clustering of the differentially expressed genes and pathway determination. The upregulated and downregulated genes in the radiation group were analyzed by the Database for Annotation, Visualization and Integrated Discovery online tool for Gene Ontology (GO) annotation and Kyoto Encyclopedia or Genes and Genomes (KEGG) pathway determination (8,9).

Detection of adjacent genes. NCBI Gene database was used to identify the adjacent genes, the transcription of which can be affected by the pseudogene. The transcription changes of the adjacent gene and the pseudogene PPIAP43 were calculated as the difference between radiation and the control group normalized to the control value: Fold change = (radiation-control)/control.

Detection of protein candidates interacting with the RNA transcript. The RNA transcript of the pseudogene was uploaded in the catRAPID omics 'transcript vs nucleotide-binding proteome' module of the catRAPID online toolkits (10). This tool identified a series of proteins that may bind with the target nucleotide.

MicroRNA (miRNA) determination. miRDB online (11,12) was used to align potential miRNAs with RNA transcripts of pseudogenes PPIAP43 and PPIA.

Basic Local Alignment Searching Tool (BLAST) of peptidyl-prolyl cis-trans isomerase A (PPIA) and PPIAP43. NCBI BLAST (https://blast.ncbi.nlm.nih.gov/Blast.cgi) was used to align the DNA sequences with pseudogene PPIAP43 and PPIA.

Database construction. Microsoft Access 2016 (Microsoft Corporation) was used for managing and relate the data across different tables.

Results

Screening upregulated and downregulated expression nucleotides after 2 Gy gamma radiation in each cell line. A total of 6,034 genes were displayed in Excel, and nine cell lines comprising H69, H128, H146, H187, H209, H526, D53, D114 and D153 were extracted from the dataset. PPIAP43 was upregulated by ≥2-fold in H69, H128, H146, H209 and H187 following radiation compared with non-irradiated controls, and was the only upregulated transcript in former four cell lines and one of the two in the H187 cell line (Tables I and II; Fig. 1). No ≥2-fold downregulated transcripts were identified in H69, H128, H146, H209 and H187 cells (Table II; Fig. 1). TAF15 was the only downregulated transcript in H114, whereas no upregulated transcripts were identified. In H526 and D153, no transcripts were differentially expressed. Multiple differentially expressed RNAs were only identified in D53, all of which were upregulated. These findings were based on the criterion of ≥2-fold change (Table II).

Detection of differentially expressed genes. Considering the similarity of expression change patterns among H69, H128, H146, H209 and H187 cells and the difficulty to determine discovery with the lack of adequate cell types of each expression change pattern in the other four cell lines, the cell lines were divided into two groups, with H69, H128, H146, H209 and H187 labeled group A, and H526, D53, D114 and D153 labeled group B. Group A was assessed using a t-test (with a random variance model) class comparison between the radiation and control groups paired by cell type with a $P<0.001$ nominal significance threshold of univariate tests. A total of 355 transcripts passed the filter with 259 upregulated and 96 downregulated transcripts (Fig. 2). False discovery rates (FDRs) were <0.018; the FDR of ILMN_3208715, which was annotated as PPIAP43, was $<1x10^{-7}$. Top five upregulated genes or pseudogenes in group A are presented in Table II. Group B was processed by the same algorithm; three upregulated and nine downregulated transcripts were identified on average. The transcription patterns of the two groups before and after radiation were distinguishable from each other (Fig. 3). The genes highly expressed before and after radiation in radiosensitive group A compared with group B were identified to be genes that are highly expressed in normal testis and lymph nodes. The genes highly expressed before and after radiation in radiosensitive group B compared with group A were related with the cell cycle (Table III). Although P-values of these differentially expressed genes between the radiation and control of group B were all <0.001, FDRs were >0.05, with the lowest FDR=0.0658.

GO function and KEGG pathway analysis. Upregulated and downregulated genes in group A were uploaded in DAVID. Although there were more upregulated transcripts compared with downregulated transcripts, the upregulated genes were involved in fewer (four pathways in total) and less reliable pathways (P>0.01 in all 4 pathways) (Table IVA). By contrast, 22 pathways were identified in the downregulated genes; four of these genes exhibited P<0.01 (Table IVB).

mRNA transcription from an adjacent protein-coding gene is negatively correlated with the transcription of PPIAP43.

Table I. Experimental design.

Cell line	Experiment ID of control	Experiment ID of radiation	PPIAP43 over transcribed	Group
H69	GSM1346757	GSM1346806	Yes	A
H128	GSM1346758	GSM1346808	Yes	A
H146	GSM1346769	GSM1346810	Yes	A
H187	GSM1346770	GSM1346812	Yes	A
H209	GSM1346781	GSM1346814	Yes	A
H526	GSM1346782	GSM1346816	No	B
D53	GSM1346793	GSM1346817	No	B
D114	GSM1346794	GSM1346818	No	B
D153	GSM1346805	GSM1346819	No	B

Table II. Transcripts with an up or downregulated transcriptional fold change ≥2-fold following 2 Gy gamma radiation in each small cell lung cancer cell line.

A, Upregulated transcripts

Cell line	ID	Transcript	ILMN gene	Entrez gene ID	Cytoband
H69	ILMN_3208715	ILMN_162197	PPIAP43	440063	11q22.1c
H128	ILMN_3208715	ILMN_162197	PPIAP43	440063	11q22.1c
H146	ILMN_3208715	ILMN_162197	PPIAP43	440063	11q22.1c
H209	ILMN_3208715	ILMN_162197	PPIAP43	440063	11q22.1c
H187	ILMN_3208715	ILMN_162197	PPIAP43	440063	11q22.1c
H187	ILMN_3251587	ILMN_177351	LOC100008589	100008589	
D53	ILMN_1656868	ILMN_45317	LOC23117	23117	16p12.2a
D53	ILMN_1772492	ILMN_22327	MCART1	92014	9p13.2a
D53	ILMN_1807291	ILMN_175467	CYP1A1	1543	15q24.1b
D53	ILMN_1892403	ILMN_168446	SNORD13	692084	8p12c
D53	ILMN_2070052	ILMN_25996	LOC613037	613037	16p11.2d
D53	ILMN_2075794	ILMN_169055	NLRP8	126205	19q13.42c
D53	ILMN_2117809	ILMN_17811	DUXAP3	503632	10q11.21a
D53	ILMN_2162367	ILMN_167637	DMC1	11144	22q13.1b-q13.1c
D53	ILMN_2342455	ILMN_15173	PPA2	27068	4q24d
D53	ILMN_3243664	ILMN_20243	LOC440353	440353	16p11.2d
D53	ILMN_3304111	ILMN_347878	LOC729978	729978	16p13.13b
D53	ILMN_3310491	ILMN_388662	MIR1978	100302173	

B, Downregulated transcripts

Cell line	ID	Transcript	ILMN Gene	Entrez gene ID	Cytoband
D114	ILMN_1678707	ILMN_18523	TAF15	8148	17q12b

Pearson correlation analysis of transcriptional changes between PPIAP43 and ARHGAP42 showed the correlation coefficient was -0.584 (P=0.099) suggesting that there was no statistically significant correlation between transcriptional changes of PPIAP43 and ARHGAP42. The adjacent transcription effects of the pseudogene PPIAP43 on the only nearby coding gene Rho GTPase activating protein 42 (ARHGAP42) were limited, as previous studies suggested that the transcription of lncRNA is positively correlated with transcription of nearby protein-coding genes if there is an effect on adjacent protein-coding genes by lncRNA transcription (13,14). The transcription levels of PPIAP43 and ARHGAP42 changed in opposite directions following radiation (Fig. 4). Of note, no P-value of the expression of ARHGAP42 in the original dataset was <0.01, which may be a limitation of this evaluation.

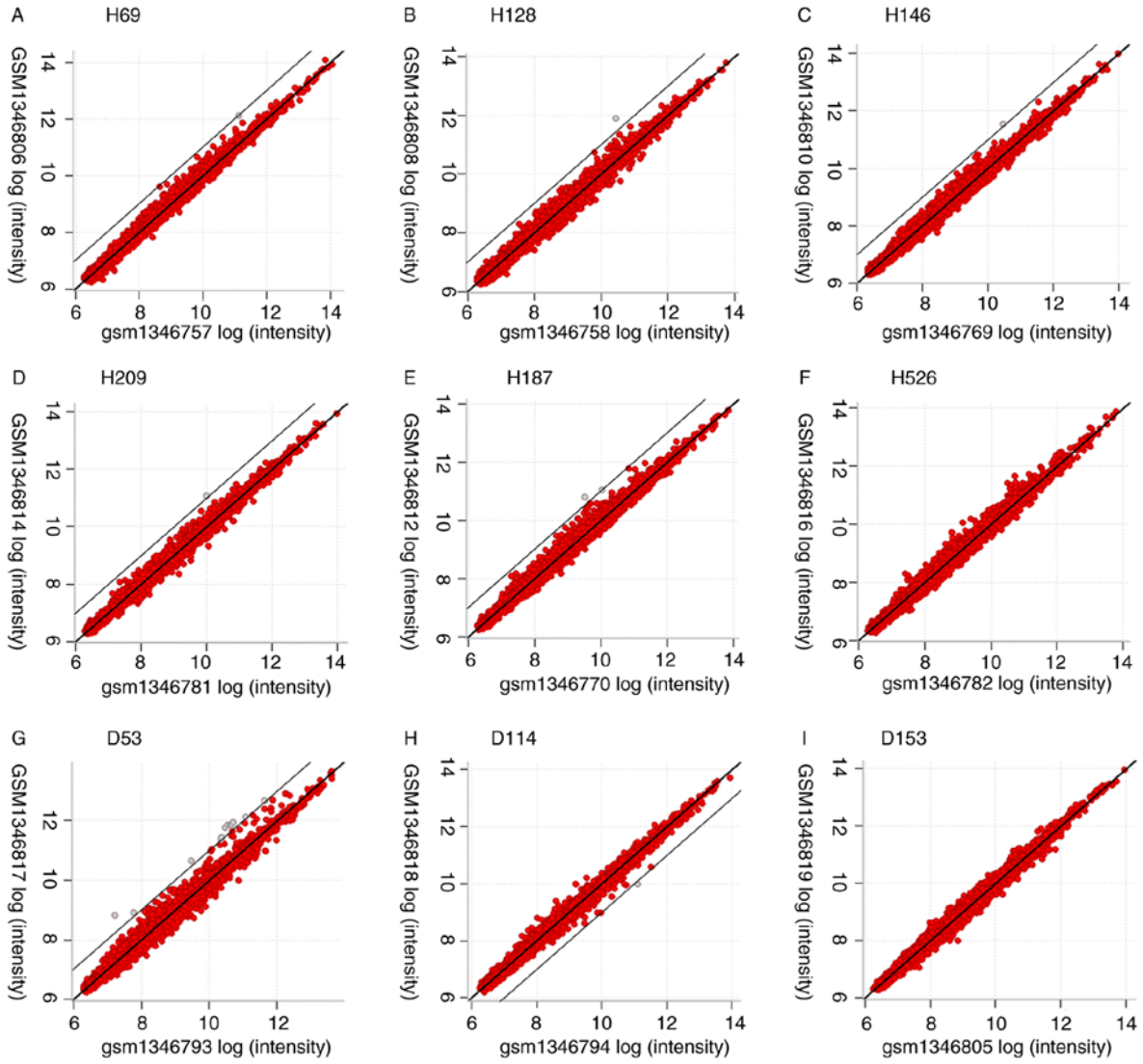

Figure 1. Genes with an up or downregulated transcriptional fold change ≥2 following irradiation with 2 Gy gamma radiation compared with unirradiated controls. PPIAP43 was the only upregulated transcript in cell line (A) H69, (B) H128, (C) H146 and (D) H209, and (E) one of the two in H187. (F) No genes were upregulated or downregulated in H526. (G) Multiple differentially expressed RNAs were identified in D53, all of which were upregulated. (H) TAF15 was the only downregulated transcript in D114, whereas no upregulated transcripts were detected. (I) No genes were upregulated or downregulated in D153. The results were based on ≥2-fold change. The white circles represent the genes and pseudogenes of which up or downregulation of transcription was ≥2-fold following irradiation with 2 Gy gamma radiation compared with unirradiated controls. The red circles represent the represent the genes and pseudogenes with <2 fold change in expression following irradiation. PPIAP43, PPIAP43, peptidyl-prolyl cis-trans isomerase A pseudogene 43; TAF15, TATA-box binding protein-associated factor 15.

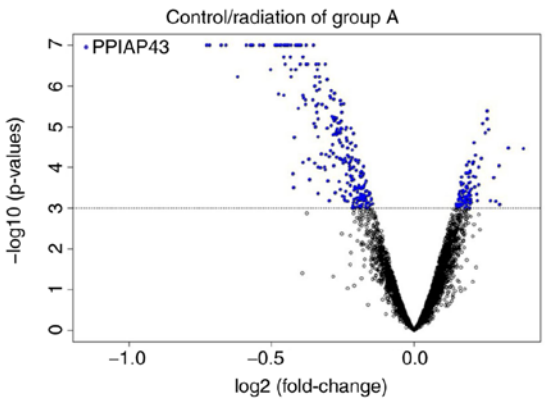

Figure 2. Differentially expressed genes and pseudogenes in control vs. radiation groups of cell lines in group A ($P<0.001$; FDR<0.018). The far top left point corresponds to PPIAP43 ($P<1x10^{-7}$; FDR<$1x10^{-7}$). PPIAP43, PPIAP43, peptidyl-prolyl cis-trans isomerase A pseudogene 43; FDR, false discovery rate.

Proteins predicted to interact with the identified lncRNA. The sequence of the RNA transcript of PPIAP43 was uploaded to the catRAPID omics 'transcript vs. nucleotide-binding proteome' module of the catRAPID online toolkits (http://service.tartaglialab.com/page/catrapid_group). The identified 118 proteins as candidates that may bind with the RNA transcript of PPIAP43. Of these, nine proteins, including TIAR, SRS10, SRSF2, TRA2B, TIA1, SFPQ, SRSF7, SRSF9 and PCBP2 were marked by catRAPID omics with necessary domains and motifs for nucleotide-binding. These nine proteins were annotated by DAVID to serve functions in nucleotide binding and splicing proteins (Table V).

BLAST of PPIA and the pseudogenes. Two aligned sections (3732 to 3917 and 5327 to 5657 of the PPIA gene sequence with identities of 96 and 94%, respectively) were identified on RNA

Table III. Differentially expressed genes with different probes consecutively expressed before and after radiation.

UniqueID	Gene name	Before P-value	Before fold change	After P-value	After fold change	Function
ILMN_2231003	MAGEA12	0.000993	0.28	0.000689	0.25	Highly expressed in normal testis
ILMN_2412880	CSAG3B	0.000009	0.32	0.000011	0.31	Highly expressed in normal testis, lymph node and spleen
ILMN_1718107	MAGEA12	0.000288	0.30	0.000376	0.32	Highly expressed in normal testis
ILMN_1761122	CSAG3B	0.000030	0.39	0.000028	0.40	Highly expressed in normal testis, lymph node and spleen
ILMN_2297352	CSAG3B	0.000026	0.45	0.000078	0.48	Highly expressed in normal testis, lymph node and spleen
ILMN_3260910	CSAG3	0.000014	0.56	0.000060	0.54	Highly expressed in normal testis, lymph node and spleen
ILMN_1803852	LOC653297	0.000528	0.59	0.000693	0.61	Similar to CSAG3B
ILMN_2328813	DMAP1	0.000198	1.85	0.000290	1.84	Transcription repression and activation
ILMN_1740319	IFI27L2	0.000195	2.23	0.000454	1.99	Apoptosis
ILMN_1810486	RAB34	0.000659	2.57	0.000836	2.33	Repositioning of lysosomes and the activation of macropinocytosis
ILMN_3238560	IFI27L2	0.000095	2.68	0.000137	2.64	Apoptosis
ILMN_1708006	MICB	0.000798	3.28	0.000683	3.14	Stress-induced self-antigen
ILMN_1796712	S100A10	0.000095	3.96	0.000187	3.80	Cell cycle progression and differentiation
ILMN_2046730	S100A10	0.000024	7.34	0.000036	6.95	Cell cycle progression and differentiation

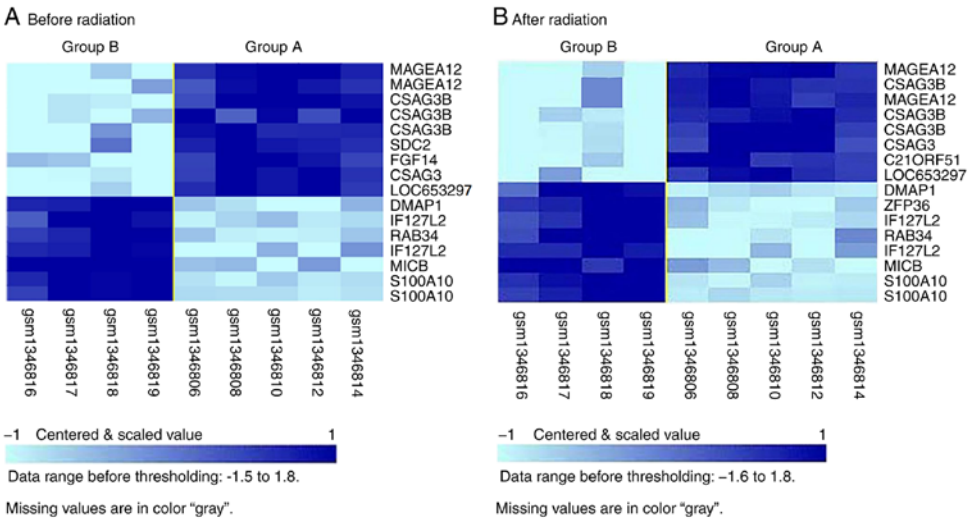

Figure 3. Differentially expressed genes with different gene probes: ILMN_2231003, ILMN_1718107 for MAGEA12; ILMN_2297352, ILMN_1761122, ILMN_2412880 for CSAG3B; ILMN_1784553 for SDC2; ILMN_1732976 for FGF14; ILMN_3260910 for CSAG3; ILMN_1803852 for LOC653297; ILMN_2328813 for DMAP1; ILMN_1740319, ILMN_3238560 for IFI27L2; ILMN_1810486 for RAB34; ILMN_1708006 for MICB; ILMN_1796712, ILMN_2046730 for S100A10; ILMN_2356311 for C21ORF51; ILMN_1720829 for ZFP36, were consecutively expressed (A) before and (B) after radiation.

Table IV. Pathways of upregulated and downregulated genes in group A after radiation.

A, pathways of upregulated genes

Category	Term	Count	%	P-value	List total	Fold enrichment
KEGG_PATHWAY	hsa01100: Metabolic pathways	19	8.558559	0.018995	63	1.701902
KEGG_PATHWAY	hsa04110:Cell cycle	5	2.252252	0.025133	63	4.402842
KEGG_PATHWAY	hsa00270:Cysteine and methionine metabolism	3	1.351351	0.045657	63	8.620301
KEGG_PATHWAY	hsa03420:Nucleotide excision repair	3	1.351351	0.066706	63	6.969605

B, pathways of downregulated genes

Category	Term	Count	%	P-value	List total	Fold enrichment
UP_KEYWORDS	Phosphoprotein	44	55	0.000379	72	1.525258
UP_KEYWORDS	Cytoplasm	29	36.25	0.001841	72	1.721256
UP_KEYWORDS	Methylation	11	13.75	0.002205	72	3.141178
UP_KEYWORDS	Alternative splicing	49	61.25	0.004189	72	1.322992
UP_KEYWORDS	Ubl conjugation	13	16.25	0.013193	72	2.179480
UP_KEYWORDS	Coated pit	3	3.75	0.013416	72	16.814542
UP_KEYWORDS	Golgi apparatus	8	10	0.021676	72	2.816229
UP_KEYWORDS	Endosome	6	7.5	0.025215	72	3.565662
UP_KEYWORDS	Cell junction	7	8.75	0.028843	72	2.964342
UP_KEYWORDS	Membrane	35	43.75	0.030912	72	1.335022
UP_KEYWORDS	Dyskeratosis congenita	2	2.5	0.037309	72	51.972222
UP_KEYWORDS	Acetylation	19	23.75	0.039913	72	1.586185
UP_KEYWORDS	Cytoskeleton	9	11.25	0.041696	72	2.260655
KEGG_PATHWAY	hsa04530: Tight junction	3	3.75	0.048329	29	8.179548
UP_KEYWORDS	Endocytosis	3	3.75	0.065530	72	7.087121
INTERPRO	IPR012677: Nucleotide-binding, alpha-beta plait	4	5	0.067759	67	4.196970
UP_KEYWORDS	Microtubule	4	5	0.072561	72	4.083532
UP_KEYWORDS	Autophagy	3	3.75	0.074222	72	6.596474
UP_KEYWORDS	Ribonucleoprotein	4	5	0.082570	72	3.862800
UP_KEYWORDS	Oxidation	2	2.5	0.089138	72	21.173868
UP_KEYWORDS	Isopeptide bond	8	10	0.094746	72	2.020122
KEGG_PATHWAY	hsa04611: Platelet activation	3	3.75	0.097433	29	5.474005

transcripts of PPIAP43 and PPIA, with the second aligned section (5327 to 5657) located primarily in the 3'-untranslated region (UTR) of PPIA mRNA (Table VI). In addition, PPIA pseudogenes PPIAP33, PPIAP80, PPIAP35 which were also upregulated by radiation, were aligned with PPIA in two sections similar to PPIAP43.

miRNA binding with PPIAP43 and PPIA or peptidyl-prolyl cis-trans isomerase A like 4A (PPIAL4A). A total of 12 and 28 miRNAs were predicted to be able to bind with the RNA transcripts of PPIAP43 and PPIA, respectively. By contrast, only one miRNA hsa-miR-876-3p, whose binding ability had been confirmed by 91 RNA-seq reads from 21 experiments, was predicted to be able to bind with PPIAP43 and PPIA. There was one binding site on PPIAP43 (target score, 74/100) and three binding sites on PPIA (target score, 92/100) (Table VI). Two of the PPIA binding sites were on pre-mRNA, and one was on the 3'UTR. By contrast,

Table V. Annotation of protein candidates to bind with the RNA transcript of PPIAP43.

Category	Term	Count	P-value	Genes	Pop hits	FDR
GOTERM_MF_DIRECT	GO:0000166~nucleotide binding	6	<0.001	SRSF2, SRSF7, SFPQ, TIA1, SRSF9, TRA2B	253	<0.001
GOTERM_BP_DIRECT	GO:0048025~negative regulation of mRNA splicing, via spliceosome	3	<0.001	SRSF7, SRSF9, TRA2B	14	0.0132
GOTERM_MF_DIRECT	GO:0036002~pre-mRNA binding	2	0.0036	SRSF2, TRA2B	6	2.1484
GOTERM_MF_DIRECT	GO:0044822~poly(A) RNA binding	4	0.0089	SRSF7, TIA1, SRSF9, POP1	789	5.2146
GOTERM_BP_DIRECT	GO:0000381~regulation of alternative mRNA splicing, via spliceosome	2	0.0136	SRSF2, TRA2B	28	9.5745

FDR, false discovery rate; SRSF2, serine and arginine rich splicing factor 2; SRSF7, serine and arginine rich splicing factor 7; SFPQ, splicing factor proline and glutamine rich; TIA1, t-cell-restricted intracellular antigen-1; SRSF9, serine and arginine rich splicing factor 9; TRA2B, transformer 2 beta homolog; POP1, processing of precursors 1.

Table VI. MicroRNAs with the ability to bind with the RNA transcript of PPIAP43 and mRNAs of PPIA and PPIAL4A.

Gene name	miRNA	PPIAP43 transcript target score	PPIAP43 transcript target site number	Gene transcript target score	mRNA target site number	Binding locations
PPIA	hsa-miR-876-3p	74	1	92	1	5485 (3'UTR)
PPIAL4A	hsa-miR-4288	79	1	87	1	151
PPIAL4A	hsa-miR-4456	72	1	52	1	597
PPIAL4A	hsa-miR-1825	59	2	55	2	194, 290

PPIA, peptidyl-prolyl cis-trans isomerase A; PPIAL4A, peptidyl-prolyl cis-trans isomerase A like 4A; PPIAP43, peptidyl-prolyl cis-trans isomerase A pseudogene 43; miR, miRNA, microRNA.

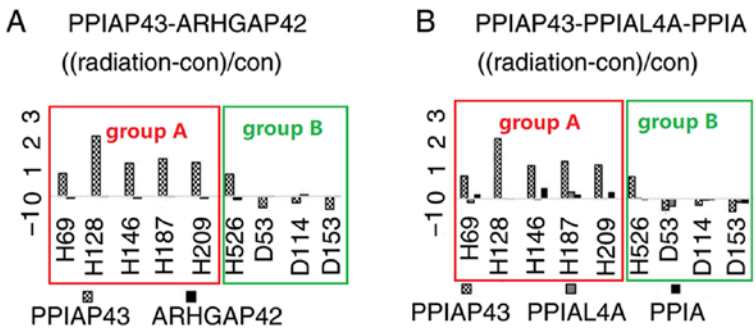

Figure 4. Transcriptional changes of PPIAP43, ARHGAP42, PPIAL4A and PPIA following irradiation with 2 Gy gamma radiation in each cell line. (A) Fold change of PPIAP43 and its adjacent gene ARHGAP42 transcripts in cell lines. (B) Fold change of PPIAP43, PPIAL4A and PPIA transcripts; the values were calculated as the difference between radiation and control group normalized to the control value as follows: Fold change = (radiation-control)/control. PPIA, peptidyl-prolyl cis-trans isomerase A; PPIAL4A, peptidyl-prolyl cis-trans isomerase A like 4A; PPIAP43, peptidyl-prolyl cis-trans isomerase A pseudogene 43; ARHGAP42, Rho GTPase activating protein 42; con, control.

three miRNAs were predicted to bind with RNA transcripts of PPIAP43 and PPIAL4A (Table VI). Transcription changes of PPIAP43, PPIA and PPIAL4A following radiation are presented in Fig. 4.

Table VII. Survival fractions of cell lines after 2 Gy radiation.

Cell line	PPIAP43 over-transcribed	Group	Survival fraction after 2 Gy γ-radiation (3)	Survival fraction after 2 Gy X-radiation (10)
H69	Yes	A		0.23
H146	Yes	A	0.6	
H187	Yes	A		0.18
H209	Yes	A		0.37
H526	No	B		0.72
D153	No	B	0.7	

PPIAP43, peptidyl-prolyl cis-trans isomerase A pseudogene 43.

Discussion

Radiation therapy remains a major form of treating patients with SCLC. However, radio-sensitivity amongst different SCLC cell lines vary. Therefore, identifying potential biomarkers for predicting radio-sensitivity, may help predict a patient's response to this mode of treatment. The results of the present study identified a lncRNA transcribed from pseudogene PPIAP43, which was overexpressed in several SCLC cell types (group A) following 2 Gy gamma radiation by ≥2-fold compared with the non-irradiated control group by bioinformatic processing of a GEO dataset. In addition, other SCLC cell lines (group B) exhibited no gene upregulation following radiation. Although the statuses of cytotoxicity column were 'YES' in groups A and B in the table of experiment descriptors displayed by the BRB ArrayTools, the original study using this GEO dataset demonstrated that the survival fraction of cell line H146 in group A and D153 in group B were ~60 and 70%, respectively (Table VII) (6). Another previous study revealed that the 2 Gy X-RAY survival fractions of H69, H187 and H209 were 0.23, 0.18 and 0.37, respectively, compared with 0.72 in H526 cells (Table VII) (15). These two studies demonstrated that the survival fractions following 2 Gy ionized radiation in cell lines in group A were lower compared with those in group B, although survival fraction values varied based on the irradiation type, cell type and other factors. These results suggest that the radiation sensitivity was different in the two groups. Therefore, the transcription change models of PPIAP43 before and after radiation may serve as a potential marker for classifying the two groups of SCLC cell lines into high and low sensitivity groups.

Further investigation revealed that pseudogene PPIAP43 was located on 11q22.1, and the only nearby protein-coding gene, which may be affected by transcription of PPIAP43, was ARHGAP42. Previous studies demonstrated that lncRNA may affect the transcription of adjacent genes by targeting activators and repressors of mRNA transcription (13,14). According to these results, PPIAP43 may affect the transcription of its adjacent gene ARHGAP42 by binding with nucleotide-binding proteins. However, Pearson's correlation analysis of transcriptional changes between PPIAP43 and ARHGAP42 was -0.584, with significance of 0.099; with former studies suggesting that the transcription of lncRNA is positively correlated with transcription of nearby protein-coding genes if there is an effect on adjacent protein-coding genes by lncRNA transcription (13,14), which indicated that PPAP43 did not statistically affect ARHGAP42 on a transcriptional level.

Another functional role of PPIAP43 is competing endogenous RNA. In this model, the RNA transcript of a pseudogene may act as a decoy to target and capture miRNAs, which can bind with RNAs of the pseudogenes and their gene counterparts (16,17). For example, in the case of the RNA of pseudogene phosphatase and tensin homolog pseudogene 1 (PTENP1), the expression level of the tumor suppressor gene PTEN is upregulated when the PTENP1 RNA is upregulated which results in decreased cancer cell proliferation; similarly, the expression level of the oncogene B-Raf proto-oncogene is upregulated when PTEN pseudogene 1 RNA is upregulated, which leads to increased proliferation of cancer cells (13,14). In the present study, an aligned section on PPIA mRNA and RNA transcript of PPIAP43 to which miRNA could bind was identified. In addition, miRNA hsa-miR-876-3p was predicted by miRDB to be capable of binding with PPIA and PPIAP43 (18-26). The binding ability of this miRNA has been confirmed by 21 experiments (18-26).

In addition, increase of RNA transcript PPIAP43 lead to upregulation of RNA transcript of PPIA. The upregulated transcription of other PPIA pseudogenes in the studied cell lines also suggested that the cross-talk between PPIA RNA and its pseudogenes mediated by miRNAs may be the dominant function pattern of PPIAP43. This suggests that under radiation stress, radiation-sensitive cells may generate more free radicals including hydroxyl radicals (27-29) compared with insensitive cells, therefore upregulating expression of PPIA (30). With the decoy effect of upregulated RNAs of PPIA pseudogenes, the binding between miRNAs and the mRNA of PPIA is decreased, the survival of PPIA mRNA is prolonged, and therefore the expression of PPIA protein is increased (17). Cyclosporine can bind with PPIA (also termed Cyclophilin A, CyPA) and other cyclophilins to suppress organ rejection by coupling with cyclosporin (31). Overexpression of PPIA is associated with poor response to inflammatory disease, cancer metastasis progression and aging (32). In lung cancer, exogenous PPIA protein stimulates H446 cell growth, whereas PPIA knockdown may lead to slower growth, decreased proliferation and increased apoptosis in cell lines ADLC-5M2 and LC-103H (25,26,33,34). Therefore, the overexpressed RNAs of PPIAP43 and other PPIA pseudogenes may serve as a remedy for reactive oxygen

species (ROS) accumulation induced by ionizing radiation to rescue the sensitive cancer cells by the decoy effect on miRNAs. In addition, there may be other resistance mechanisms used by less radio-sensitive cell types in group B. Nevertheless, the upregulated transcription of PPIAP43 and the slightly down-regulated PPIA transcription in H526 cells suggests that this cell type may be classified as high-sensitivity, although the upregulated transcriptional change of PPIAP43 in H526 was <2-fold following irradiation. This may have been due to the different conditions of gamma ray, from which transcription data was collected, and X-ray, from which the survival fraction data was collected, although there may be other influencing factors that still need to be identified.

There were certain limitations to the present *in silico* study. First, the transcription levels of PPIAP43 in the H526 cell line was not as distinct compared with those in the cell lines in group A as compared with the levels in the other cell lines in group B. Second, the survival fractions of the cell lines were obtained from different studies with incomplete information. Third, epigenetics may be also involved in the function of PPIAP43 (35), which was not considered in the present study.

A previous study demonstrated that an increased Ki-67 proliferation index may represent a predictive factor for increased tumor radio-sensitivity (36). The present study identified a potential radio-sensitivity indicator for SCLC cell lines following early radiation *in vitro*. The results of this study revealed that a ≥2-fold transcriptional change of pseudogene PPIAP43 following irradiation with 2 Gy gamma radiation may represent a predictive factor for increased tumor radio-sensitivity. To describe this association in detail, additional studies with more cell types and experimental methods are required. Further *in vivo* studies, particularly studies involving blood tests, may provide a basis to use the lncRNA identified in the present study to help early identification of less radiation-sensitive SCLC types and reduce the unnecessary radiation side effects in patients with SCLC.

Acknowledgements

Not applicable.

Funding

This study was supported by The National Key Research and Development Program of China (grant. no. 2018YFC1313200).

Availability of data and materials

The datasets used and/or analyzed during the present study are available from the corresponding author on reasonable request.

Authors' contributions

JY conceived and designed the study. SW conducted the experiment and analysis, and drafted the manuscript. JY and SW reviewed, edited and approved the manuscript.

Ethics approval and consent to participate

Not applicable.

Patient consent for publication

Not applicable.

Competing interests

The authors declare that they have no conflicts of interest.

References

1. Gazdar AF, Bunn PA and Minna JD: Small-cell lung cancer: What we know, what we need to know and the path forward. Nat Rev Cancer 17: 725-737, 2017.
2. Sabari JK, Lok BH, Laird JH, Poirier JT and Rudin CM: Unravelling the biology of SCLC: Implications for therapy. Nat Rev Clin Oncol 14: 549-561, 2017.
3. Hendricks MV, Sheils WC and Davis WB: Radiation-induced lung injury. Clin Pulm Med 6: 287-295, 1999.
4. Videtic GM, Stephans KL, Woody NM, Pennell NA, Shapiro M, Reddy CA and Djemil T: Stereotactic body radiation therapy-based treatment model for stage I medically inoperable small cell lung cancer. Pract Radiat Oncol 3: 301-306, 2013.
5. Jassem J: The rote of radiotherapy in lung cancer: Where is the evidence? Radiother Oncol 83: 203-213, 2007.
6. Owonikoko TK, Zhang G, Deng X, Rossi MR, Switchenko JM, Doho GH, Chen Z, Kim S, Strychor S, Christner SM, *et al*: Poly (ADP) ribose polymerase enzyme inhibitor, veliparib, potentiates chemotherapy and radiation in vitro and in vivo in small cell lung cancer. Cancer Med 3: 1579-1594, 2014.
7. Simon R, Lam A, Li MC, Ngan M, Menenzes S and Zhao Y: Analysis of gene expression data using BRB-ArrayTools. Cancer Inform 3: 11-17, 2007.
8. Huang da W, Sherman BT and Lempicki RA: Systematic and integrative analysis of large gene lists using DAVID bioinformatics resources. Nat Protoc 4: 44-57, 2009.
9. Huang da W, Sherman BT and Lempicki RA: Bioinformatics enrichment tools: Paths toward the comprehensive functional analysis of large gene lists. Nucleic Acids Res 37: 1-13, 2009.
10. Bellucci M, Agostini F, Masin M and Tartaglia GG: Predicting protein associations with long noncoding RNAs. Nat Methods 8: 444-445, 2011.
11. Wong N and Wang X: miRDB: An online resource for microRNA target prediction and functional annotations. Nucleic Acids Res 43: D146-D152, 2015.
12. Wang X: Improving microRNA target prediction by modeling with unambiguously identified microRNA-target pairs from CLIP-ligation studies. Bioinformatics 32: 1316-1322, 2016.
13. Goodrich JA and Kugel JF: Non-coding-RNA regulators of RNA polymerase II transcription. Nat Rev Mol Cell Biol 7: 612-616, 2006.
14. Luo S, Lu Y, Liu L, Yin Y, Chen C, Han X, Wu B, Xu R, Liu W, Yan P, *et al*: Divergent lncRNAs regulate gene expression and lineage differentiation in pluripotent cells. Cell Stem Cell 18: 637-652, 2016.
15. Carmichael J, Degraff WG, Gamson J, Russo D, Gazdar AF, Levitt ML, Minna JD and Mitchell JB: Radiation sensitivity of human-lung cancer cell-lines. Eur J Cancer Clin Oncol 25: 527-534, 1989.
16. Karreth FA, Reschke M, Ruocco A, Ng C, Chapuy B, Léopold V, Sjoberg M, Keane TM, Verma A, Ala U, *et al*: The BRAF pseudogene functions as a competitive endogenous RNA and induces lymphoma in vivo. Cell 161: 319-332, 2015.
17. Poliseno L, Salmena L, Zhang J, Carver B, Haveman WJ and Pandolfi PP: A coding-independent function of gene and pseudogene mRNAs regulates tumour biology. Nature 465: 1033-1038, 2010.
18. Griffiths-Jones S, Grocock RJ, van Dongen S, Bateman A and Enright AJ: miRBase: MicroRNA sequences, targets and gene nomenclature. Nucleic Acids Res 34: D140-D144, 2006.
19. Landgraf P, Rusu M, Sheridan R, Sewer A, Iovino N, Aravin A, Pfeffer S, Rice A, Kamphorst AO, Landthaler M, *et al*: A mammalian microRNA expression atlas based on small RNA library sequencing. Cell 129: 1401-1414, 2007.
20. Lam LT, Lu X, Zhang H, Lesniewski R, Rosenberg S and Semizarov D: A MicroRNA screen to identify modulators of sensitivity to BCL2 inhibitor ABT-263 (Navitoclax). Mol Cancer Ther 9: 2943-2950, 2010.

21. Wang RYL, Weng KF, Huang YC and Chen CJ: Elevated expression of circulating miR876-5p is a specific response to severe EV71 infections. Sci Rep 6: 24149, 2016.
22. Bao L, Lv L, Feng J, Chen Y, Wang X, Han S and Zhao H: MiR-876-5p suppresses epithelial-mesenchymal transition of lung cancer by directly down-regulating bone morphogenetic protein 4. J Biosci 42: 671-681, 2017.
23. Ayub Khan SM, Few LL and See Too WC: Downregulation of human choline kinase α gene expression by miR-876-5p. Mol Med Rep 17: 7442-7450, 2018.
24. Kozomara A and Griffiths-Jones S: miRBase: Integrating microRNA annotation and deep-sequencing data. Nucleic Acids Res 39: D152-D157, 2011.
25. Xu Q, Zhu Q, Zhou Z, Wang Y, Liu X, Yin G, Tong X and Tu K: MicroRNA-876-5p inhibits epithelial-mesenchymal transition and metastasis of hepatocellular carcinoma by targeting BCL6 corepressor like 1. Biomed Pharmacother 103: 645-652, 2018.
26. Wang Y, Xie Y, Li X, Lin J, Zhang S, Li Z, Huo L and Gong R: MiR-876-5p acts as an inhibitor in hepatocellular carcinoma progression by targeting DNMT3A. Pathol Res Pract 214: 1024-1030, 2018.
27. Joiner MC and van der Kogel A (eds): Basic Clinical Radiobiology 5th Edition. CRC Press/Taylor & Francis Group (Boca Raton, FL, USA), pp 188-205, 2019.
28. Wallace SS: Enzymatic processing of radiation-induced free radical damage in DNA. Radiat Res 150 (5 Suppl): S60-S79, 1998.
29. Riley PA: Free radicals in biology: Oxidative stress and the effects of ionizing radiation. Int J Radiat Biol 65: 27-33, 1994.
30. Suzuki J, Jin ZG, Meoli DF, Matoba T and Berk BC: Cyclophilin A is secreted by a vesicular pathway in vascular smooth muscle cells. Circ Res 98: 811-817, 2006.
31. Matsuda S and Koyasu S: Mechanisms of action of cyclosporine. Immunopharmacology 47: 119-125, 2000.
32. Nigro P, Pompilio G and Capogrossi MC: Cyclophilin A: A key player for human disease. Cell Death Dis 4: e888, 2013.
33. Yang H, Chen J, Yang J, Qiao S, Zhao S and Yu L: Cyclophilin A is upregulated in small cell lung cancer and activates ERK1/2 signal. Biochem Biophys Res Commun 361: 763-767, 2007.
34. Howard BA, Furumai R, Campa MJ, Rabbani ZN, Vujaskovic Z, Wang XF and Patz EF Jr: Stable RNA interference-mediated suppression of Cyclophilin A diminishes non-small-cell lung tumor growth in vivo. Cancer Res 65: 8853-8860, 2005.
35. Sanchez-Elsner T, Gou D, Kremmer E and Sauer F: Noncoding RNAs of trithorax response elements recruit Drosophila Ash1 to ultrabithorax. Science 311: 1118-1123, 2006.
36. Ishibashi N, Maebayashi T, Aizawa T, Sakaguchi M, Nishimaki H and Masuda S: Correlation between the Ki-67 proliferation index and response to radiation therapy in small cell lung cancer. Radiat Oncol 12: 16, 2017.